Supporting Information

Chlorin e6 and polydopamine modified Gold nanoflowers for combined photodynamic and photothermal therapy

Fengren Wu,[ab] Yongjia Liu,[b] Yan Wu [a] Dianwen Song,[c] Jiwen Qian[a] and Bangshang Zhu[*ab]

[a] School of Chemistry and Chemical Engineering, Shanghai Jiao Tong University, Shanghai 20040, China;

[b] Instrumental Analysis Center, Shanghai Jiao Tong University, Shanghai, 20040, China

[c] Department of Orthopedics, Shanghai General Hospital, School of Medicine, Shanghai Jiao Tong University, Shanghai, 201620, China.

[*] Corresponding author. E-mail address: bshzhu@sjtu.edu.cn (Bangshang Zhu)

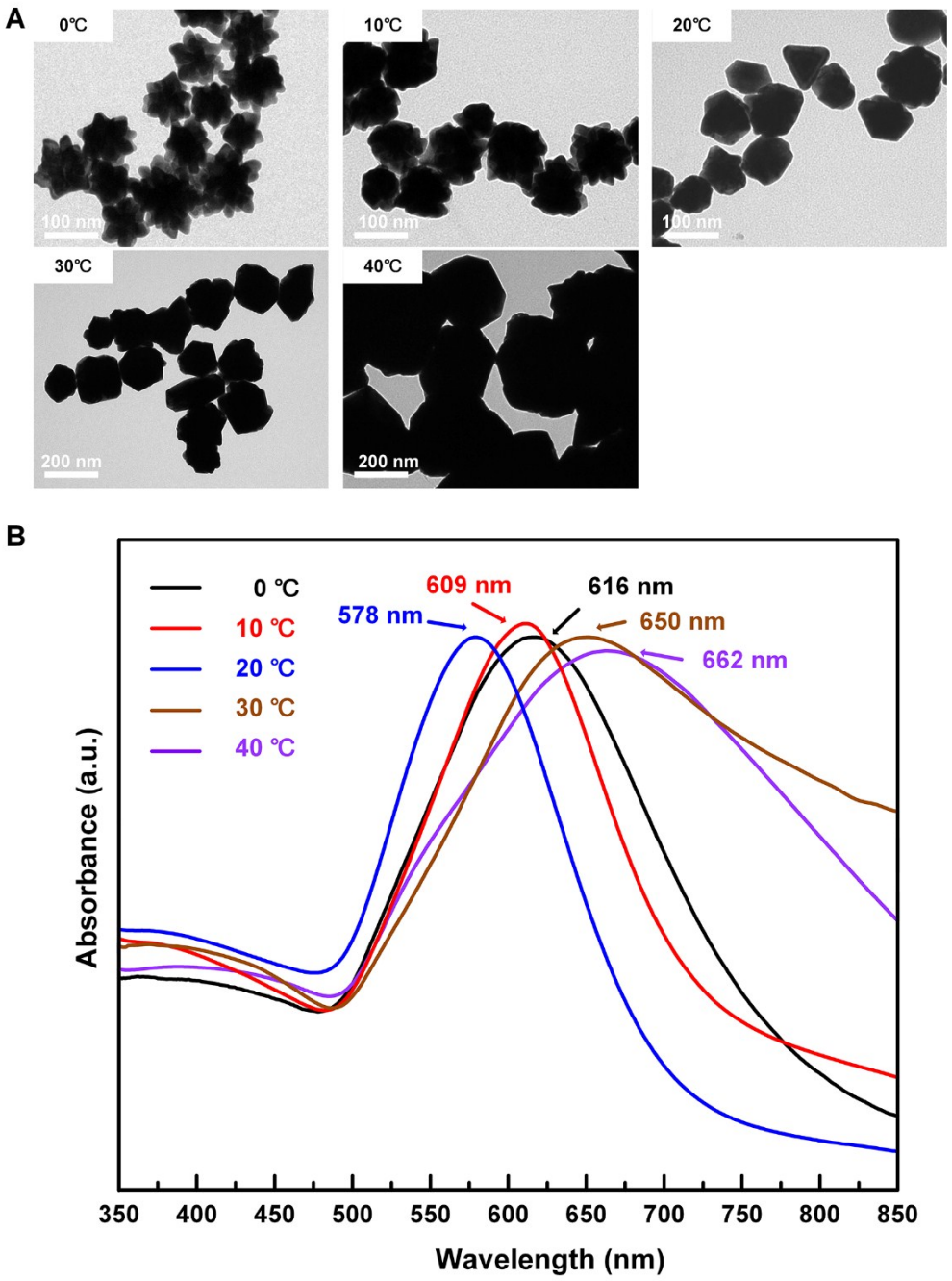

Fig. S1. (A) TEM images and (B) Vis-NIR spectra of AuNFs synthesized under the temperature of 0, 10, 20, 30 and 40 °C.

AuNFs were synthesized at the temperature of 0, 10, 20, 30 and 40 °C, respectively. When the temperature was changed from low to high, the nanoparticle morphology was changed as well, the size of AuNFs became larger and the branched spikes got fewer and fewer until disappeared. It was found that the optimal reaction temperature was 0 °C.

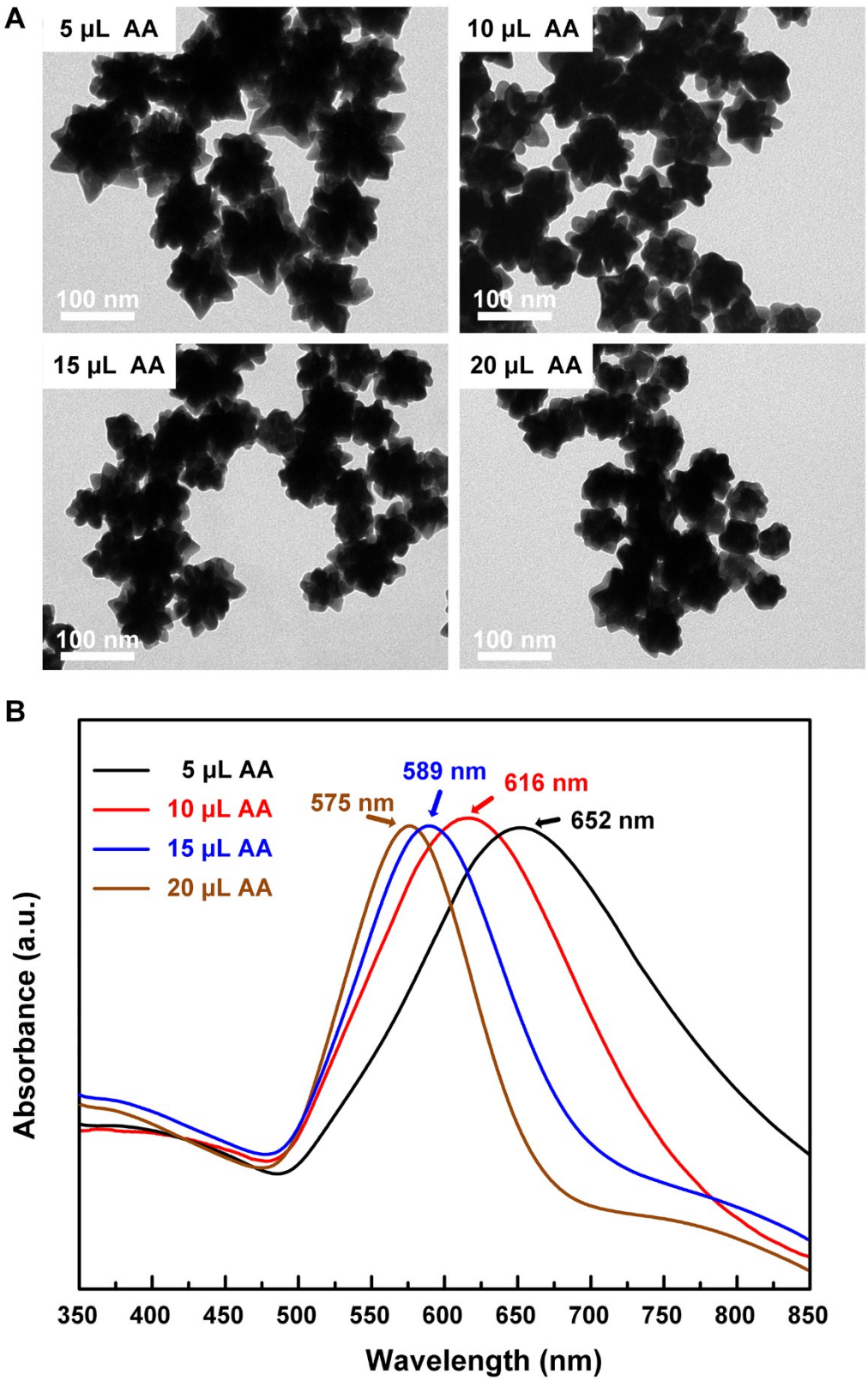

Fig. S2. (A) TEM images and (B) Vis-NIR spectra of AuNFs affected by different amounts of AA: 5, 10, 15, and 20 μL AA.

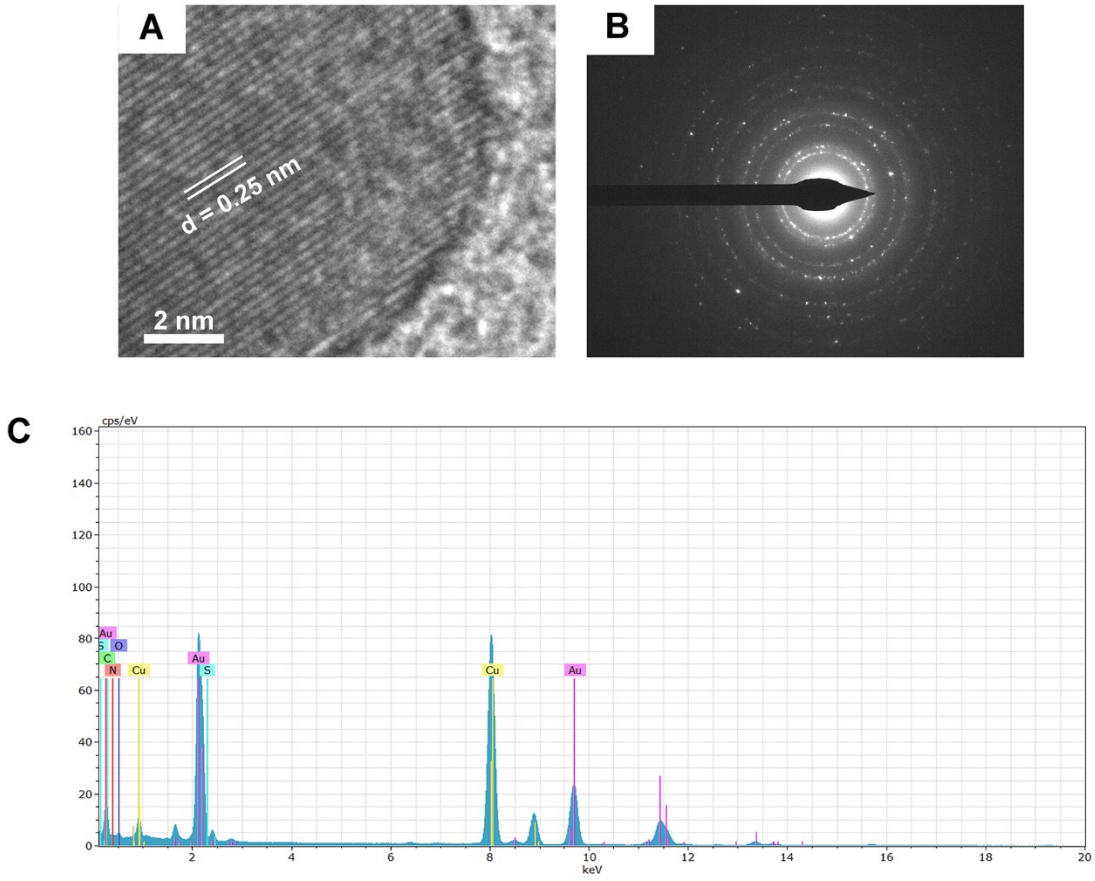

Fig. S3. (A) HRTEM, (B) SAED images and (C) EDS spectroscopy for elemental analysis of PDA-Ce6-GSH-AuNFs including C, N, O, S and Au.

HRTEM image demonstrated that protrusions with random orientation deriving from solid dark core are crystalline, while the selected area electron diffraction (SAED) images further proved the polycrystalline character of AuNFs. The energy dispersive spectrum (EDS) for elemental analysis confirmed the presence of organic layer outside the AuNFs in PDA-Ce6-GSH-AuNFs.

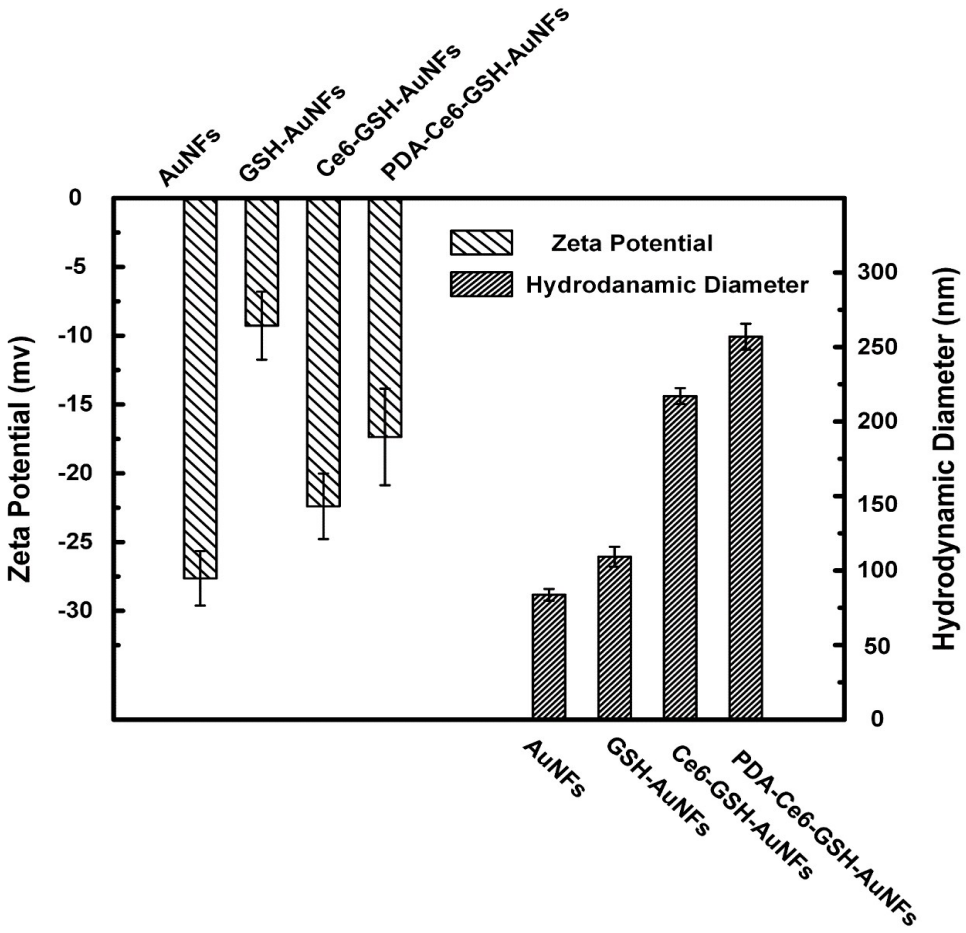

Fig. S4. The Zeta potential and hydrodynamic diameter of AuNFs, GSH-AuNFs, Ce6-GSH-AuNFs and PDA-Ce6-GSH-AuNFs.

The dynamic light scattering analysis data indicated that the hydrodynamic diameter of GSH-AuNFs was 109.26 ± 6.72 nm, a little larger than AuNFs (83.75 ± 3.92 nm), and the hydrodynamic diameter of Ce6-GSH-AuNFs was increased to 217.09 ± 5.38 nm. The size of PDA-Ce6-GSH-AuNFs was 257 ± 8.67 nm.

The Zeta potential of AuNFs, GSH-AuNFs, Ce6-GSH-AuNFs and PDA-Ce6-GSH-AuNFs were -27.64 ± 1.98 mV, -9.27 ± 2.47 mV, –22.4 ± 2.38 mV and –17.36 ± 3.51 mV.

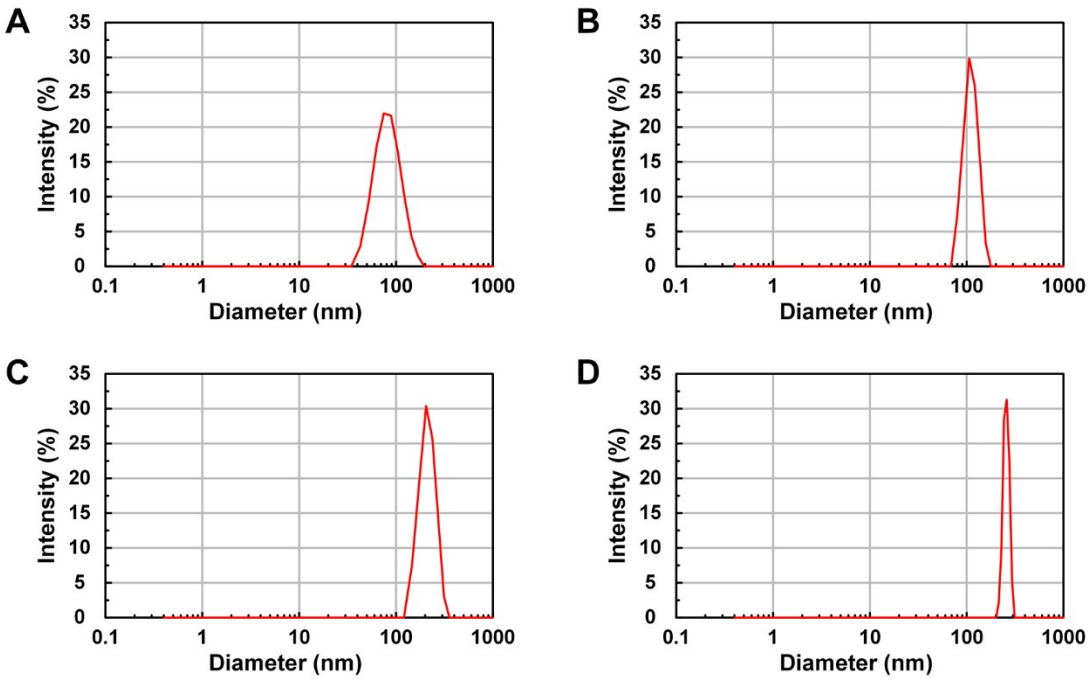

Fig. S5. Size distribution of (A) AuNFs, (B) GSH-AuNFs, (C) Ce6-GSH-AuNFs and (D) PDA-Ce6-GSH-AuNFs.

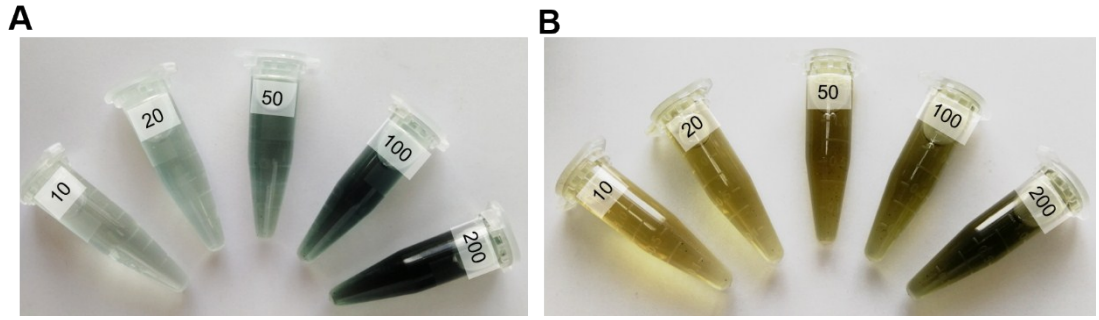

Fig. S6. PDA-Ce6-GSH-AuNFs dispersed in (A) PBS (pH=5.8) and (B) FBS with different concentrations: 10, 20, 50, 100 and 200 μg/mL.

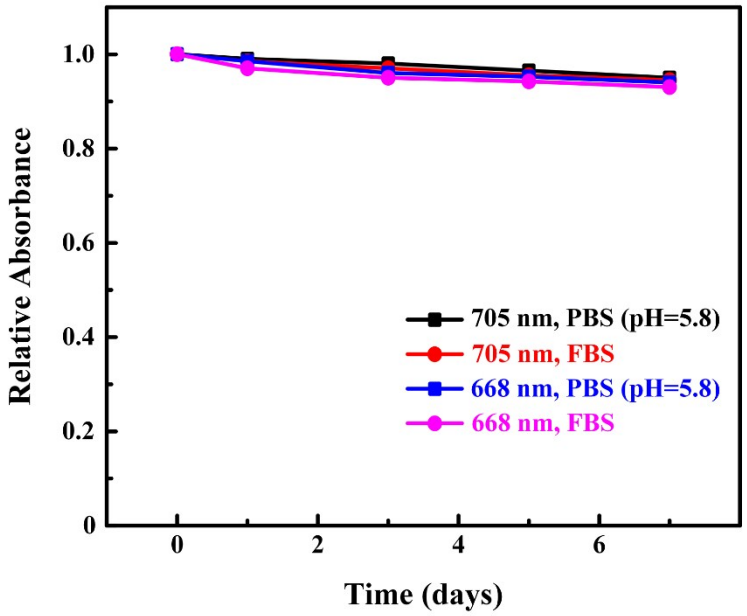

Fig. S7. The NIR absorbance of the 705 nm and 668 nm peaks of PDA-Ce6-GSH-AuNFs dispersed in PBS (pH=5.8) and FBS at 0, 1, 3, 5 and 7 days, normalized to the initial absorbance.

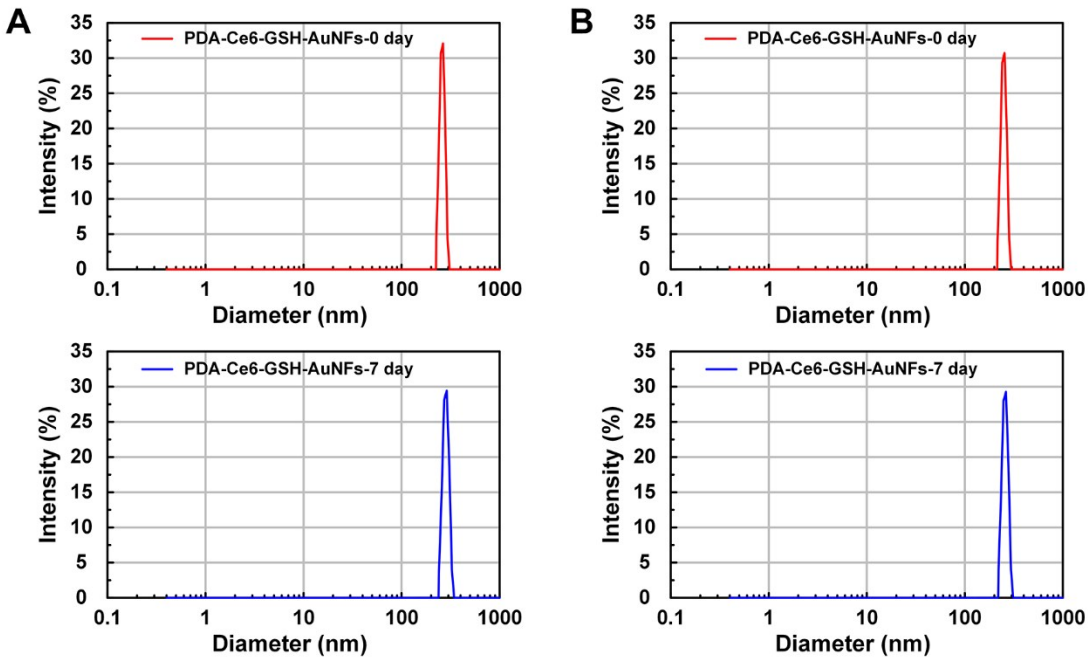

Fig. S8. DLS analysis results of PDA-Ce6-GSH-AuNFs dispersed in (A) PBS (pH=5.8) and (B) FBS at 0 and 7 days.

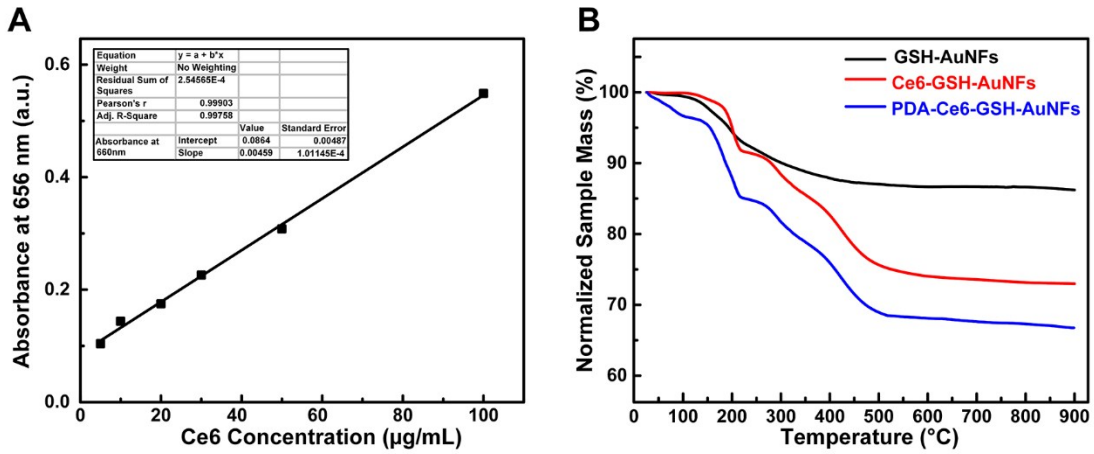

Fig. S9. (A) The standard curve of Ce6 in PBS. The concentration of Ce6 in solution were 5, 10, 15, 20, 30, 50 and 100 μg/mL, respectively. (B) TGA curves of GSH-AuNFs, Ce6-GSH-AuNFs and PDA-Ce6-GSH-AuNFs.

Tab. S1. The weight remained of AuNFs, GSH, Ce6 and PDA at 500 and 900 ˚C calculated according to TGA curves presented in Fig. S9B.

T/Mass	AuNFs	GSH	Ce6	PDA
500 (˚C)	67.2 wt.%	10.5 wt.%	13.6 wt.%	8.7 wt.%
900 (˚C)	66.4 wt.%	10.5 wt.%	14.0 wt.%	9.1 wt.%

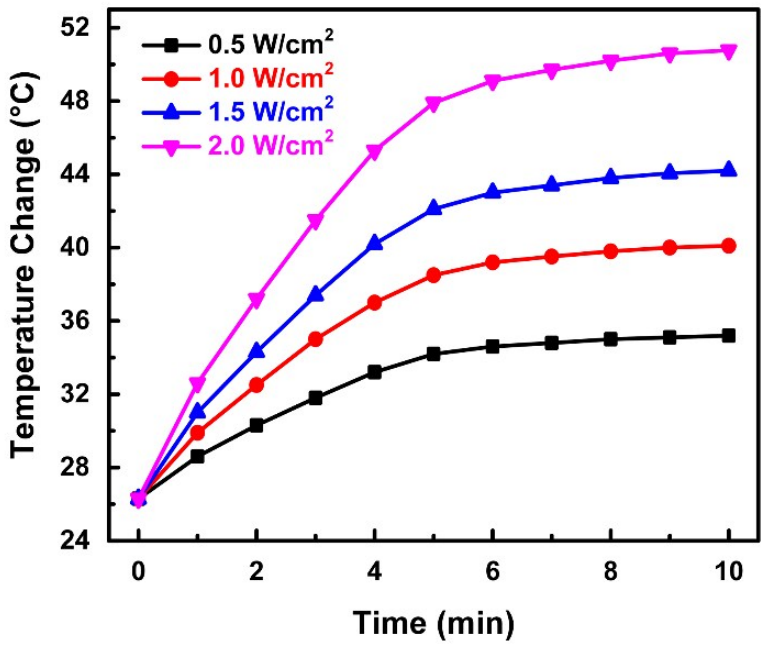

Fig. S10. Temperature elevation of PDA-Ce6-GSH-AuNFs (200 μg/mL) solutions at different power density (0.5, 1.0, 1.5 and 2.0 W/cm^2) for 10 min.

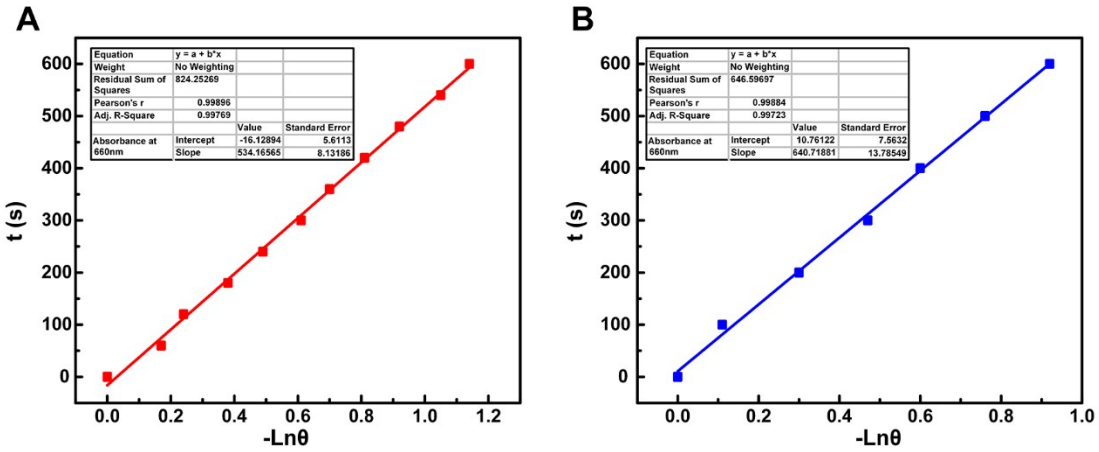

Fig. S11. Determination of the time constant of (A) AuNFs and (B) PDA-Ce6-GSH-AuNFs for heat transfer from the system using a linear regression of the cooling profile.

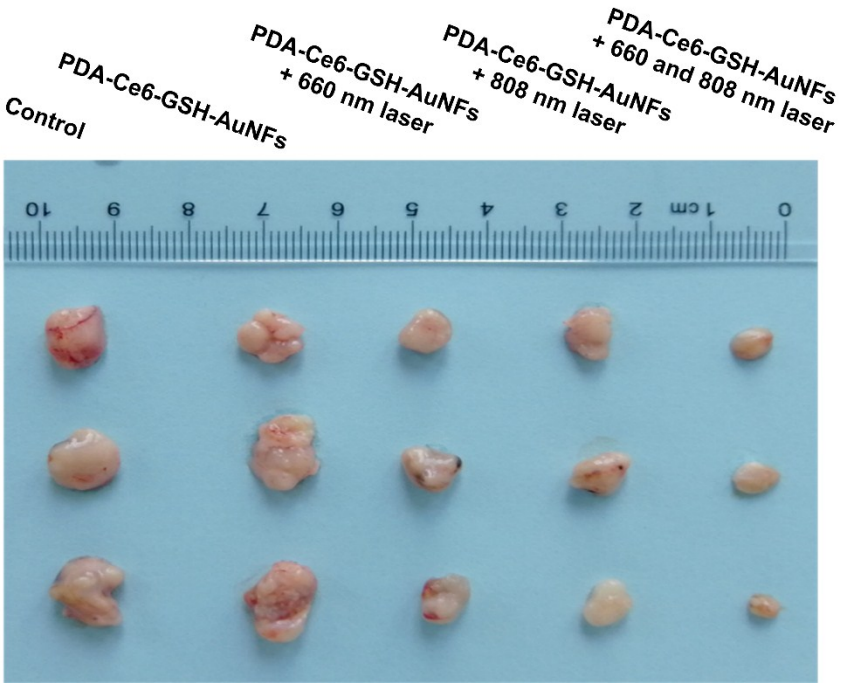

Fig. S12. Images of excised tumors from each group after post treatment.